REPORT DOCUMENTATION PAGE

Form Approved
OMB No. 0704-0188

1. REPORT DATE *(DD-MM-YYYY)*	2. REPORT TYPE	3. DATES COVERED *(From - To)*
3/10/2008	Final Report	1/15/05 – 12/31/2007

4. TITLE AND SUBTITLE
FA9550-05-1-0054
Diatomaceous, Fungal, and Bacterial Building Blocks for Materials Synthesis

5a. CONTRACT NUMBER
N/A

5b. GRANT NUMBER
FA9550-05-1-0054

5c. PROGRAM ELEMENT NUMBER
N/A

6. AUTHOR(S)
Chad A. Mirkin, PI

5d. PROJECT NUMBER
N/A

5e. TASK NUMBER
N/A

5f. WORK UNIT NUMBER
N/A

7. PERFORMING ORGANIZATION NAME(S) AND ADDRESS(ES)
Northwestern University
633 Clark Street, 2-502 Crown Plaza
Evanston, IL 60208-1110

8. PERFORMING ORGANIZATION REPORT NUMBER
N/A

9. SPONSORING / MONITORING AGENCY NAME(S) AND ADDRESS(ES)
Dr. Hugh De Long /NL
Air Force Office of Scientific Research
875 N. Randolph Street, Suite 325, Room 3112
Arlington, VA 22203-1768

10. SPONSOR/MONITOR'S ACRONYM(S)
AFOSR

11. SPONSOR/MONITOR'S REPORT NUMBER(S)

12. DISTRIBUTION / AVAILABILITY STATEMENT
N/A

Approved for public release. Distribution is unlimited

AFRL-SR-AR-TR-08-0217

13. SUPPLEMENTARY NOTES
N/A

14. ABSTRACT

This final report provides a summary of the scientific and technological breakthroughs achieved during the 3 years of this project. It includes a list of publications, participation in scientific meetings, workshops, and lectures, and invention disclosures. The project was extremely productive as the highlights of the scientific and technological accomplishments in this report will show. The objectives of this project were: (1) To develop methods for controlling the interaction between nanoparticles and microorganism templates to allow the rational assembly of micro- and macroscopic materials with properties tailored at the nanoparticle level; (2) to align and organize nanoparticle/microorganism composite materials three-dimensionally on surfaces to allow full exploitation of their unique properties; (3) to develop novel nanoparticle structures with unusual properties that can be used in materials assembly, and (4) to characterize and evaluate the electrical transport, photovoltaic, and spectroscopic enhancement properties. During the three years of this grant significant progress was made towards all four objectives. With respect to using diatoms as templates for the development of new nanomaterials, a method was developed to generate nanostructured metallic microshells using microorganism precursors. The electronic properties of these metallic microshells were investigated, and a method developed to assemble various nanoparticles onto microorganism surfaces to exploit the properties of these nanoparticles for applications in microelectronics. It was also shown that these microshells can serve as substrates for the detection of analytes using surface enhanced Raman scattering (SERS).

15. SUBJECT TERMS
Diatoms, nanoparticle/microorganism composite materials, microshells, anisotropic functionalization, gold nanoaparticles , surface enhanced Raman scattering (SERS)

16. SECURITY CLASSIFICATION OF:			17. LIMITATION OF ABSTRACT	18. NUMBER OF PAGES	19a. NAME OF RESPONSIBLE PERSON
a. REPORT	b. ABSTRACT	c. THIS PAGE			19b. TELEPHONE NUMBER *(include area code)*

AFOSR FINAL REPORT

DIATOMACEOUS, FUNGAL, AND BACTERIAL BUILDING BLOCKS FOR MATERIAL SYNTHESIS

Award Number: FA9550-05-1-0054

Principal Investigator:
Chad A. Mirkin
Department of Chemistry
Northwestern University
2145 Sheridan Road
Evanston, IL 60208

chadnano@northwestern.edu
Phone:(847) 491-2907
Fax: (847) 467-5123

April 8, 2008

Period Covered by this Report: 1/1/05-12/31/07

OBJECTIVES AND STATUS OF WORK

This final report provides a summary of the scientific and technological breakthroughs achieved during the 3 years of this project. It includes a list of publications, participation in scientific meetings, workshops, and lectures, and invention disclosures. The project was extremely productive as the highlights of the scientific and technological accomplishments in this report will show.

The objectives of this project were: (1) To develop methods for controlling the interaction between nanoparticles and microorganism templates to allow the rational assembly of micro- and macroscopic materials with properties tailored at the nanoparticle level; (2) to align and organize nanoparticle/microorganism composite materials three-dimensionally on surfaces to allow full exploitation of their unique properties; (3) to develop novel nanoparticle structures with unusual properties that can be used in materials assembly, and (4) to characterize and evaluate the electrical transport, photovoltaic, and spectroscopic enhancement properties. During the three years of this grant significant progress was made towards all four objectives.

With respect to using diatoms as templates for the development of new nanomaterials, a method was developed to generate nanostructured metallic microshells using microorganism precursors. The electronic properties of these metallic microshells were investigated, and a method developed to assemble various nanoparticles onto microorganism surfaces to exploit the properties of these nanoparticles for applications in microelectronics. It was also shown that these microshells can serve as substrates for the detection of analytes using surface enhanced Raman scattering (SERS). In addition to our studies on metallic microshells, two new techniques for the synthesis of asymmetrically functionalized nanoparticles were developed. These techniques allowed us to design and assemble unique nanoparticle heterostructures. The first technique took advantage of the differences in the T_m of different DNA duplexes, whereas the second method was geometrically based and used the enzyme T4-DNA ligase. During the last funding year the latter technique was significantly improved and a protocol developed that allowed us to control the number of extended strands per nanoparticle as a function of the amount of enzyme used and the number of template magnetic microparticles (MMP) recycled. A third approach consisted of exploring nanoparticle conjugates functionalized with membrane active peptides and antisense oligonucleotides as a new platform for gene targeting and expression studies. Experiments performed with these particles demonstrated a significant advance in the use of nanoparticle-biomolecule conjugates for intracellular applications. It was shown that (1) gold nanoparticles could be functionalized with two different biomolecules, (2) the density of each molecule could be easily controlled, and (3) both functionalities remained active in both *in vitro* and *in vivo* systems.

ACCOMPLISHMENTS

A.1. Diatoms as Templates for the Development of New Nanomaterials

Microorganisms can be used as versatile templates for the assembly of nanostructured building blocks into larger functional architectures. Diatoms, a diverse class of unicellular algae with unique shapes and complex cell walls composed of silica, have for many years attracted the interest of biologists and materials scientists. There are literally thousands of taxonomically different diatoms available in nature that can be distinguished based on their intricate silica shell, called frustule. Frustules, which are composed of two halves that fit tightly into each other, have dimensions between 1 to 100 μm. Recently scientists have begun to explore the possibility of using diatoms as templates for the development of new nanomaterials. We have previously shown that diatoms can serve as templates for the formation of metallic microshells that display the full range of nanostructural details of diatom cell walls. For these experiments and the studies described in this report diatoms belonging to two taxonomically different classes, *Synedra* and *Thalassiosira,* were utilized. Briefly, metal-coated diatom frustules were generated from pure *Synedra* and *Thalassiosira* diatom cultures grown in either freshwater (*Synedra*) or silicate-rich growth medium (*Thalassiosira*). Scheme 1 outlines schematically the preparation of nanostructured metallic microshells using diatom templates. Diatoms of both classes were first subjected to Piranha digestion to remove the organic components. After removal of the organic components, the remaining silica frustules were deposited as a non-overlapping monolayer onto a Piranha-cleaned glass substrate (Scheme 1) and either Ti metal (5 nm) or Ag metal (30 nm) evaporated onto the diatom-coated substrate. Scanning electron microscopy (SEM) (Figure 1) of the three-dimensional metal-coated diatom frustules revealed that the silver coating was deposited homogeneously across the diatom surfaces and that the morphology as well as the intricate nanoscopic features of the diatom templates were maintained (Figure 1 b,d).

Scheme 1. Preparation of nanostructured metallic microshells from diatom templates

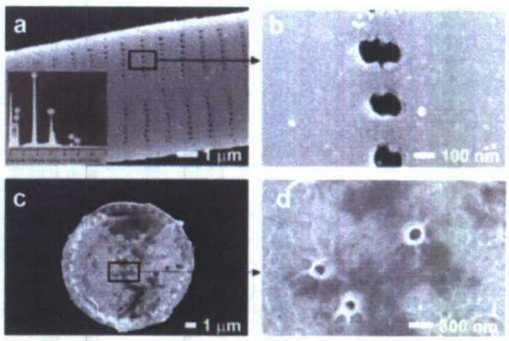

Figure 1. Metal-coated diatom frustules **(a)** and **(b)** Synedra; **(c)** and **(d)** Thalassiosira.

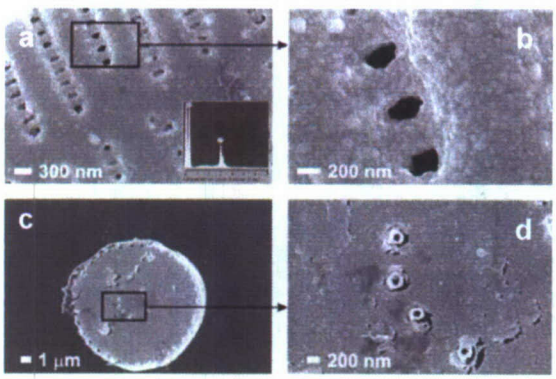

Figure 2. Metallic microshell replicas of diatom frustules. **(a)** and **(b)** Synedra; **(c)** and **(d)** Thalassiosira.

After dissolution/etching of the diatom templates using HF, metallic microshell

replicas that have retained the structural identity of the respective diatom templates and thus carried the full range of nanostructural details present on the respective template surfaces, were isolated (Figure 2). Most important, the 30 nm thick silver microshell is rather robust and remains intact throughout the etching process. The fabrication process outlined in Scheme 1 is important for several reasons. Since the templates are unicellular organisms that exist in thousands of structurally unique shapes and uniquely patterned cell walls composed of nanospecific details, one has ample opportunity to choose as template a species with the desired details. Second, our synthetic process is straightforward, high-yielding, easily reproducible, and can be performed with a variety of metals and metal compositions, depending on the desired application. Lastly, the resulting three-dimensional free-standing products exhibit nanostructural detail including regularly patterned sub-200 nm pore sizes. Thus, diatoms can act as sacrificial templates for the formation of three-dimensional nanostructured metallic microshells.

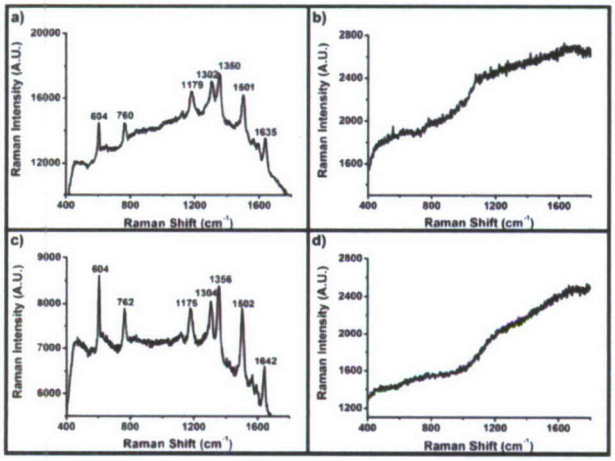

Figure 3. SERS spectra of R6G using as substrates silver-coated *Synedra* frustules. **(a)** 1 mM, **(b)** 1 μM R6G. SERS spectra of R6G using as substrates silver-coated *Thalassiosira* frustules. **(c)** 1 mM, **(d)** 1 μM R6G.

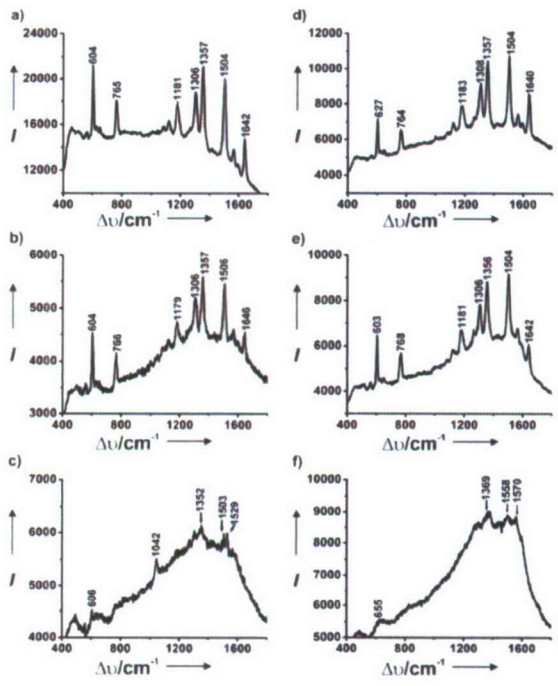

Figure 4. SERS spectra of R6G using as substrates *Synedra*-templated metallic microshells. **(a)** 1mM, **(b)** 1μM, **(c)** 100 nM R6G. SERS spectra of R6G using as substrates *Thalassiosira*-templated metallic microshells. **(d)** 1mM, **(e)** 1 μM, **(f)** 100 nM R6G.

Both, the silver-coated diatoms and silver microshell diatom replicas, (Figures 2b, d; 3b, d) display distinct sub-100 nm topological features that were not observed when 30 nm of Ag was evaporated onto a glass microscope cover slip, indicating that the fused silica particles comprising the underlying structure of the diatom frustules are responsible for the observed roughness of the resulting metallic materials. Since roughened metal surfaces and silver colloids are effective SERS substrates, it was hypothesized that the diatom-templated metallic materials could potentially be used as substrates for the optical detection of analytes using SERS. As a first step in this direction, the SERS activity of the silver-coated diatom frustules was investigated (Figure 4). In both cases, *Synedra* as well as *Thalassiosira*, only 1mM rhodamine 6G

concentrations gave detectable SERS signals. Assuming 100 % coverage of the silver-coated diatom substrate by the dye, the enhancement factor was calculated to be approximately $4x10^5$ and $2x10^5$ for *Synedra* and *Thalassiosira* as templates, respectively. When identical SERS experiments were performed on the isolated silver microshells, the SERS signal intensity for the 1 mM solution increased dramatically, and a significant signal was recorded for both, the 1 μM and 100 nM, solutions (Figure 4) with enhancement factors of $1x10^6$ and $7x10^5$ for the *Synedra* and *Thalassiosira* templates, respectively, more than twice the intensity observed for the silver-coated diatom frustules. This striking increase in SERS intensity upon template removal can in part, though not entirely, be attributed to an increase in the exposed metal surface area with which the Raman dye can associate. A second contributing factor to the observed increase in SERS intensity is the potential impact HF treatment might exert on the SERS signal since a similar effect has been reported for other mineral acids and anions.

A.2. Electrical Properties of Metallic Microshells

It was previously shown that diatoms can serve as templates for the assembly of nanoparticles and for the formation of metallic microshells that display the full range of nanostructured details of the diatom cell walls. During the past year the electronic properties of these metallic microshells were investigated and a method developed to assemble a variety of nanoparticles on silica frustules. In addition, the potential use of these new materials in electronics applications was illustrated.

It was shown that diatoms can act as templates for the formation of isolable metallic microshells that exhibit the nanostructural detail of the diatom cell wall. The remaining silica frustules were then deposited as non-overlapping monolayers onto glass substrates that were carefully cleaned with Piranha solution. Ti metal (5 nm) and Au metal (30 nm) were evaporated onto the diatom-coated substrate. Scanning electron microscopy (SEM) of the 3-D products revealed that the gold coating was deposited homogeneously across the diatom surfaces and that the morphology and intricate nanoscopic features of the diatom templates were maintained. Metallic microshell replicas of the diatoms were isolated after dissolution of the diatom templates with HF. These materials were structurally identical to their respective diatom templates in so far as they had retained all of the nanostructural details of the diatom surfaces. Moreover, the 30 nm thick gold microshells were robust and remained intact throughout the etching process. In order to investigate the electrical properties of these microshells, electrical measurements were conducted

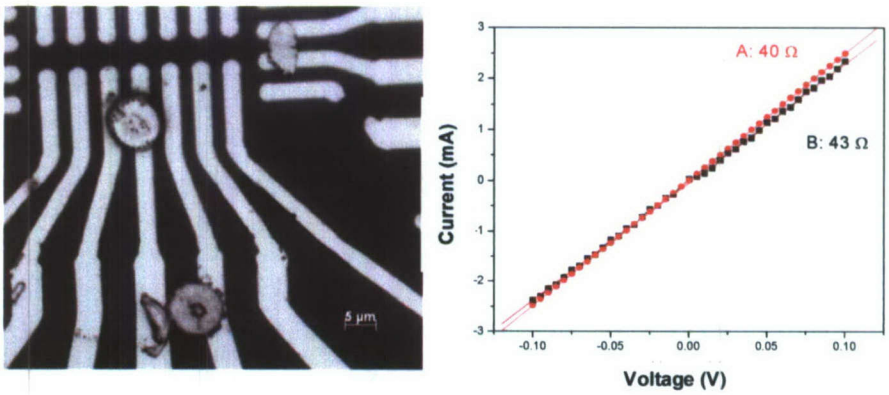

Figure 5. Microscope image of *Thalassiosira* gold microshells on microelectrode and I-V measurements for microshells.

and solutions of *Thalassiosira* gold microshells dropped onto microelectrodes fabricated using E-beam Lithography. Using microscopy techniques we were able to locate where the microshells made contact across two or more of the gold electrodes (Figure 5). The results of these experiments are summarized in Figure 5. The I-V curve at room temperature showed a linear response as is expected for bulk gold. Since these results were different from what was anticipated, it was decided to further exploit the shape of diatom frustules for use in nanoelectronics. Therefore different nanoparticles were assembled on frustules generated from pure diatom cultures grown in silicate-rich growth medium. Scheme 2 outlines schematically how gold or silver nanoparticles, and gold or silver nanoprisms were assembled onto the frustule. *Synedra* diatoms were first subjected to a Piranha digestion to remove the organic components. Once the organic components were removed, the remaining silica frustules were functionalized with positively charged poly(diallyldimethylammonium chloride or PDDA (Scheme 2). The PDDA frustules were rinsed and subsequently resuspended in various negatively charged nanoparticle solutions. Due to the electrostatic interactions, the positively charged frustules were coated by the negatively charged particles. The nanoparticle coatings produce an electrically percolating monolayer of different nanoshapes. In order to investigate how the shape influences the electrical properties, electrical measurements were conducted on these new materials, and solutions of nanoparticle functionalized diatom frustules dropped onto microelectrodes fabricated by E-beam lithography. Using microscopy techniques we were able to locate where nanoparticle functionalized diatom frustules made contact across two or more of the gold electrodes, and resistance measurements were conducted at these positions (Figure 6). Our preliminary results indicated that the resistance for the silver nanoparticle coated diatoms was 5.08 x 10^{11} Ω, while the resistance for the gold nanoparticle and gold nanoprism coated diatoms was determined to be 1.6 x 10^{12} Ω and 2.07 x 10^{12} Ω, respectively (Figure 6A and B). However, further experiments did not confirm these initial results and no differences were found between different shapes. One possible explanation could

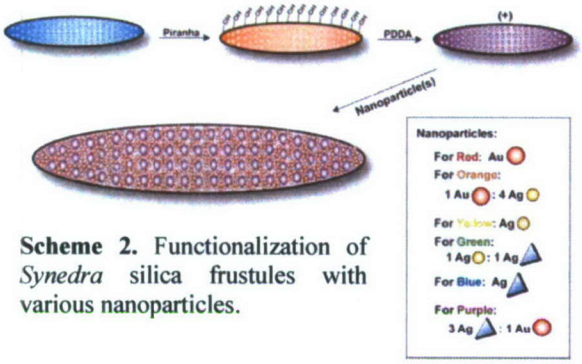

Scheme 2. Functionalization of *Synedra* silica frustules with various nanoparticles.

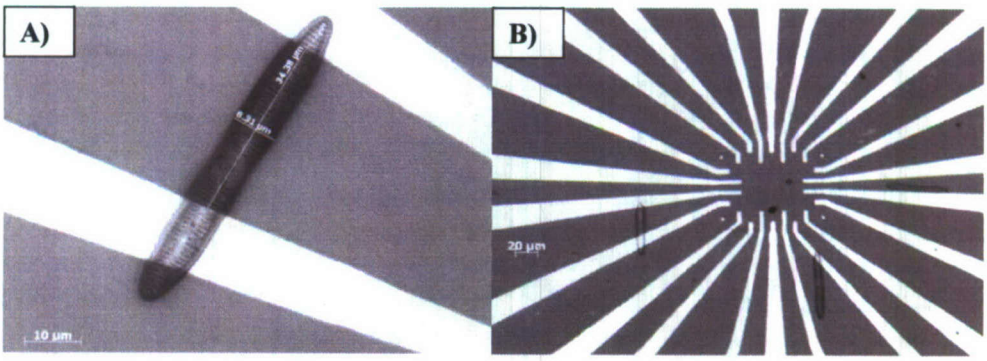

Figure 6. Microscope images of **(A)** gold nanoparticle coated, and **(B)** gold prism coated diatoms on microelectrodes.

be the concentrations of the nanoparticles on the surface and potential interferences from the silica component of the diatoms, which might have interfered with these measurements.

B. Symmetrially Functionalized Nanoparticle Building Blocks

B.1. Synthesis of Asymmetrically Functionalized Nanoparticle Building Blocks Using T4 DNA Ligase

Most nanoparticle assembly studies have focused on the use of isotropically functionalized particles since there are very few methods for selectively functionalizing different surface regions of an individual particle. However, if one could deliberately functionalize only one hemisphere or one distinct point on a particle in a general way, one could begin to introduce valency into such structures, thereby allowing greater control over the assembly process. A general strategy was developed that allowed us to functionalize gold nanoparticles (AuNP) with two different types of oligonucleotides in a site-specific manner by using a magnetic sphere as a geometric-restriction template (Scheme 3). Anisotropic functionalization of AuNPs was accomplished using a three-component assembly strategy consisting of: (1) magnetic microparticles (MMPs, 2.8-μm diameter polystyrene particles with iron oxide cores) functionalized with 3'-thiol terminated 30-mer oligonucleotides **1**, (2) 3'-hydroxyl-modified "extension" oligonucleotides **2** that are complementary to one half of the MMP oligonucleotides, and (3) AuNPs (13 nm, citrate-stabilized particles) densely functionalized with 3'-thiolated and 5'-phosphorylated 15-mer oligonucleotides **3** that are half-complementary to the other half of the MMP oligonucleotides.

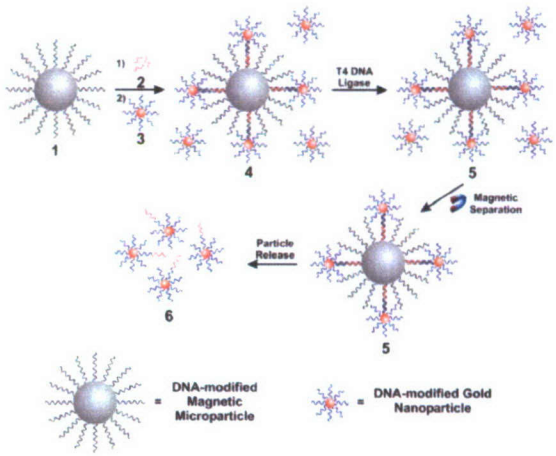

Scheme 3. Geometric strategy for the asymmetrical functionalization of AuNP.

The three components assembled in ligation buffer to form complex **4** in which the oligonucleotide-modified MMPs act as templates for co-alignment of the 3'-hydroxy group of the "extension" oligonucleotides with the 5'-phosphate group of the AuNP oligonucleotide. T4 DNA ligase was added to the reaction solution to catalyze the formation of a phosphodiester bond between the 3'- hydroxyl and the 5'-phosphate of the "extension" oligonucleotides and the oligonucleotide chemisorbed to the AuNP, respectively, thus affording new 30-mer oligonucleotides bound only to the sections of the AuNP that could hybridize with the MMP template. After ligation complex **5** was removed from the reaction mixture via magnetic separation, and the new anisotropically-modified AuNPs **6** were released from the MMP templates by heating.

As proof-of-concept 13 and 30 nm AuNPs (molar ratio

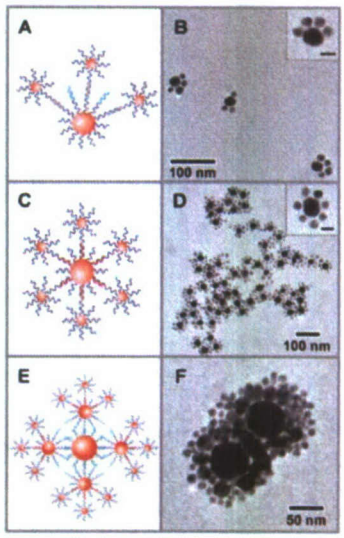

Figure 7. Directional assembly of asymmetrically-functionalized gold NPs into different structures. **(A, B)** "cat paw," **(C, D)** satellite, and **(E, F)** dendrimer-like structures.

10:1), both of which were asymmetrically functionalized with complementary extension oligonucleotides, were mixed. Because only the "extension" oligonucleotides of the AuNPs can hybridize, a "cat paw" structure was formed (Figure 7A,B), suggesting that for each 30 nm AuNP approximately 1/3 to 1/2 of its surface was asymmetrically functionalized. We also reacted asymmetrically functionalized 13 nm AuNPs with 30 nm AuNPs functionalized with oligonucleotides that were complementary only to the extended strands on the 13 nm AuNP. Due to the asymmetric functionalization of AuNP **6** (Scheme 3), the two sets of nanoparticles did not aggregate, but instead formed satellite structures consisting of one 30-nm AuNP surrounded by 13 nm AuNPs. The formation of a third type of nanostructure resembling a dendrimer is possible through these asymmetrically-functionalized particles. For example, satellite structures that resemble those in Figures 7C were prepared from 30 and 60 nm AuNPs. These dendrimer-like structures were formed by further hybridizing the non-extended oligonucleotides on the 30 nm particles with complementary extension oligonucleotides on asymmetrically-functionalized 13 nm AuNPs (Figure 7E, F). The formation of this three-component structure demonstrates that this method and asymmetrically functionalized particles can be used to precisely control the assembly of at least three different AuNPs into designed heterostructures in a step-by-step fashion.

B.2. Thermal Synthesis of Asymmetrically Functionalized AuNPs

A second strategy for the asymmetrical functionalization of AuNPs was developed. This protocol took advantage of the temperature dependence of different duplex DNA strands. The thermal approach is illustrated in Scheme 4. Briefly, DNA linkers are used to connect oligonucleotide-modified gold nanoparticles to a larger oligonucleotide-modified SiO_2 particle to form a satellite structure **5** (Scheme 4A). The resulting DNA duplexes that interconnect the satellite structure are thermally addressable at two different sites, one adjacent to the SiO_2 particle (7-mer) and the other near the gold particle (12-mer). Since these two duplexes have different lengths, they melt at different temperatures (T_ms), thus allowing one to release the gold nanoparticles with the linker intact and to yield an exposed "sticky end" **8**. In a typical procedure, 7-mer oligonucleotide-modified SiO_2 particles **1** were hybridized with a 27-mer oligonucleotide containing a 7-mer complementary region **2,** which produces particles with many duplexes possessing 20-mer overhanging ends **3**. These particles were then hybridized to gold nanoparticles functionalized with the 12-mer oligonucleotide **4**, which is complementary to the overhanging portion of **3**. The 12-mer and 7-mer duplexes melt at 35°C and 23°C, respectively, and allow one to address the structures thermally in an independent and sequential manner. When a molar ratio of gold nanoparticles to SiO_2 of 1,000:1 was used, satellite structure **5** was formed such that only a few oligonucleotides on one hemisphere of each of the nanoparticles hybridized to the central SiO_2

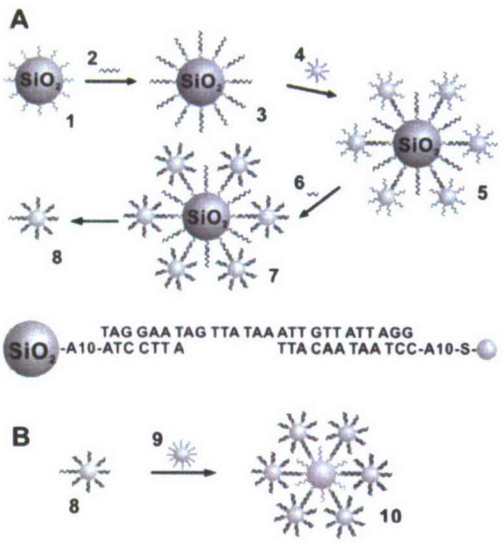

Scheme 4. Thermal strategy for the asymmetrical functionalization of AuNP.

particles. The remaining oligonucleotides on the gold nanoparticle surface were then blocked to form duplexes with the 12-mer oligonucleotide **6**. Since the T_ms of the 7-mer and 12-mer duplexes that connect the gold nanoparticles and SiO_2 particles differ by 12°C, the 7-mer regions could be selectively dehybridized by increasing the temperature above the T_m for the 7-mer duplexes while remaining below the T_m for the 12-mer structures. This temperature increase liberated the asymmetrically functionalized gold nanoparticles **8** which possessed overhanging oligonucleotides with "sticky ends" only at the points of contact between the gold nanoparticles and the larger SiO_2 particles. Transmission electron microscopy (TEM), UV-vis spectroscopy, and light-scattering measurements were carried out to characterize the assembled nanostructures. Satellite structures composed of 20 nm gold nanoparticles surrounded by several 13 nm gold particles, were characterized using TEM (Figure 8).

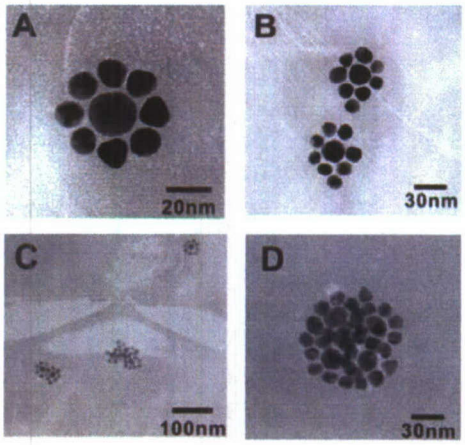

Figure 8. TEM images of 13 and 20 nm asymmetrically functionalized AuNPs.

In conclusion, this thermal synthetic strategy, which is based on the differences in the T_m of different DNA duplexes, is very general and should allow asymmetric functionalization of many important classes of nanoparticles, including semiconductor quantum dots, noble metals, and magnetic particle structures.

B.3 Synthesis of Asymmetrically Functionalized Nanoparticle Building Blocks Using T4 DNA Ligase

B.3.1. Quantitative Control over the Extent of Asymmetric Functionalization

Asymmetric functionalization has the potential to introduce valency into nanostructures, which allows greater control in assemblies of nanoparticles. In addition to established applications these structures will potentially have great value for biology. Recent research in our group has shown that oligonucleotide functionalized AuNPs can readily enter cells and perform gene knockdown. It was hypothesized that asymmetrically functionalized nanoparticles will be able to deliver agents to cells that normally could not be taken up. One way to pursue this objective is by modifying certain agents such as proteins or pharmaceuticals with oligonucleotides, followed by hybridizing them to one asymmetrically functionalized face of the nanoparticle. The other face will remain unaltered for transfection into cells.

In order to fully utilize the advantages that asymmetric functionalization can offer, a detailed characterization of the products of this system is required. The most critical parameter that needs to be determined is the extent of asymmetric functionalization, or the number of strands enzymatically added to the AuNP, which is critical to determine the amount of molecular "cargo" that can be transfected by a single AuNP.

In order to improve the consistency of the number of strands "extended" from run to run, many factors need to be addressed. The first change made to the system was the ligation buffer used in the enzymatic step, which contained components such as the surfactant sodium dodecyl sulphate (SDS) and EDTA that are detrimental to the performance of the enzyme T4 ligase. The surfactant SDS is known to change the conformation of proteins, and to denature enzymes. Also,

ligase requires divalent magnesium to function. The previous buffer, however, included EDTA, which competes with the enzyme for metal ions, thus reducing its performance. In the new buffer, which extended the enzymatic lifetime of the ligase, SDS was substituted by a milder surfactant, Tween 20, and EDTA was omitted.

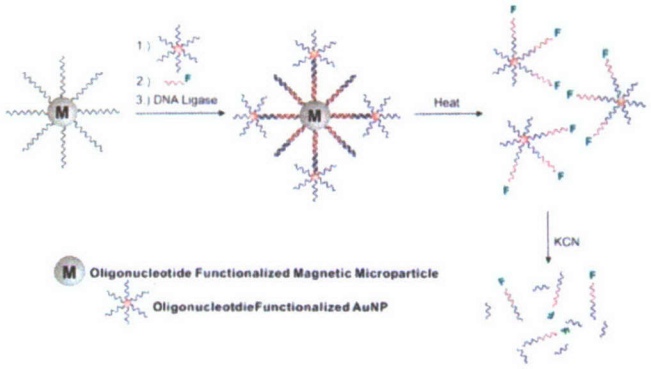

Scheme 5. Oligonucleotides conjugated to AuNPs and free oligonucleotides are hybridized to a template strand linked to a magnetic microparticle. The free strand and oligonucleotides adsorbed to the AuNP surface are enzymatically linked. The duplexes are melted and the particles are dissolved with KCN.

The next major modification to improve the consistency of asymmetric functionalization was introducing a "pre-hybridization" step that allowed the AuNP oligonucleotides, extension strands and MMP oligonucleotides to hybridize before addition of T4 ligase to the mixture. Previously, the three aforementioned components and the ligase were mixed and then incubated overnight at room temperature. During this pre-hybridization step the oligonucleotides were "primed" to be ligated together. This is a significant improvement because ligase quickly becomes inactive in the asymmetric functionalization mixture.

For quantification of the number of extended strands per AuNP, the extension strands were labeled with a fluorophore. After asymmetric functionalization, the released particles were quantified by measuring the absorbance and dissolved in KCN (Scheme 5). The number of extended strands per particle was calculated by dividing the concentration of the fluorophore by the concentration of the particles in the sample.

Two methods were developed to quantitatively control the extent of asymmetric functionalization. The first method was based on varying the addition of enzyme to the reaction mixture. Although the enzyme has a short lifetime in the reaction mixture, this could be used to control the extent of asymmetric functionalization. The second method for controlling the extent of functionalization is the number of times the template magnetic microparticles (MMP) are recycled. Figure 9 summarizes these results. Varying the amount of enzyme added and reusing the MMPs allowed us to reproducibly extend between 2 to 12 asymmetrically functionalized strands per AuNP, which in return allowed us to control the amount of cargo being transfected into cells.

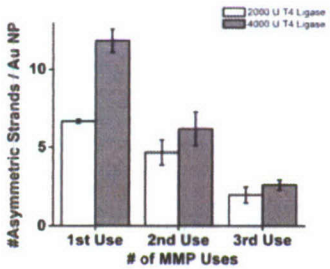

Figure 9. The number of extended strands per gold nanoparticle as a function of the amount of enzyme added and the number of times the recycled MMPs were used.

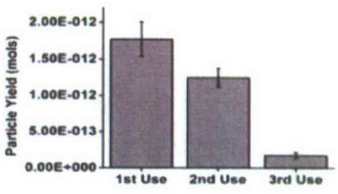

Figure 10. The yield of AuNPs as a function of the number of uses of the recycled MMP.

Next, the yield of asymmetrically functionalized product that was produced was quantified. This

quantification is critical for designing cellular uptake experiments. Figure 10 shows the yield of AuNPs asymmetrically functionalized as a function of MMP recycling. The yield of particles drops considerably with each use. These results indicate a significant advance in controlling the process of asymmetric functionalization. We predict they will have applications ranging from cellular transfection to materials assembly.

B.4. Peptide and Oligonucleotide Functionalized Gold Nanoparticles

Previously we demonstrated that oligonucleotide functionalized gold nanoparticles could be used as antisense agents. We have extended this work and synthesized and characterized nanoparticles functionalized with peptides and oligonucleotides. These particles were then used for intracellular applications. During the last funding year a new method was developed for nanoparticle conjugates functionalized with membrane active peptides and antisense oligonucleotides. These conjugates are more efficient antisense agents than previously reported nanoparticle systems.

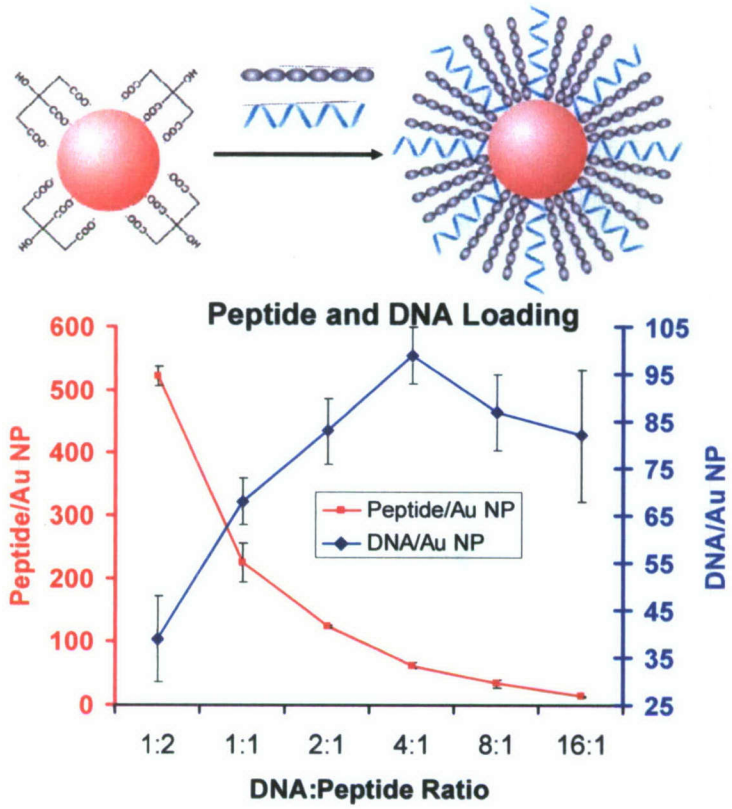

Figure 11. Peptide and DNA Functionalized Au NPs. Scheme for preparing peptide and oligonucleotide functionalized gold nanoparticles (**top**). Absolute numbers of oligonucleotides and peptides per nanoparticle at various initial ratios (**bottom**).

Gold nanoparticles were synthesized following published methods. Briefly, 0.01% Tween-20 and 0.2M NaCl were added to a solution of gold nanoparticles (13 ± 1 nm), followed by thiol terminated ss-DNA and cysteine terminated peptides. The pH was adjusted with 0.01M phosphate buffer, and the nanoparticles aged by using increasing NaCl concentrations. After separation of unbound peptides and oligonucleotides from the nanoparticle conjugates by centrifugation, the conjugates were suspended in phosphate buffer for further analysis. Next we characterized the surface loading of the conjugates with peptides and oligonucleotides using fluorescence assays. These assays showed that as the oligonucleotide loading of the particles increased, the peptide loading decreased and vice versa (Figure 11). The respective numbers for each moiety could be controlled by varying the initial ratios of peptides and oligonucleotides. For example, at an oligonucleotide to

peptide ratio of 1:1, the number of oligonucleotide and peptide strands per nanoparticle was determined to be 68 ± 5 and 225 ± 31 respectively, whereas at an oligonucleotide to peptide ratio of 2:1, the numbers were 83 ± 7 and 124 ± 7.

These conjugates were further characterized by measuring the ability of the surface bound oligonucleotide to bind its complementary partner. Fluorescein labeled complementary oligonucleotides were added to a solution containing nanoparticles functionalized with peptides and oligonucleotides. The solution was heated to 65°C, cooled to allow annealing of complementary strands, and slowly reheated. Finally the bulk fluorescence resulting from dehybridization of complementary strands was measured. When the peptide containing system was compared to the traditional oligonucleotide functionalized nanoparticle system, no difference was observed between these conjugates and the traditional oligonucleotide-only system (Figure 12) indicating that the peptides had no measurable effect on the binding properties of the oligonucleotides on the gold nanoparticle surface.

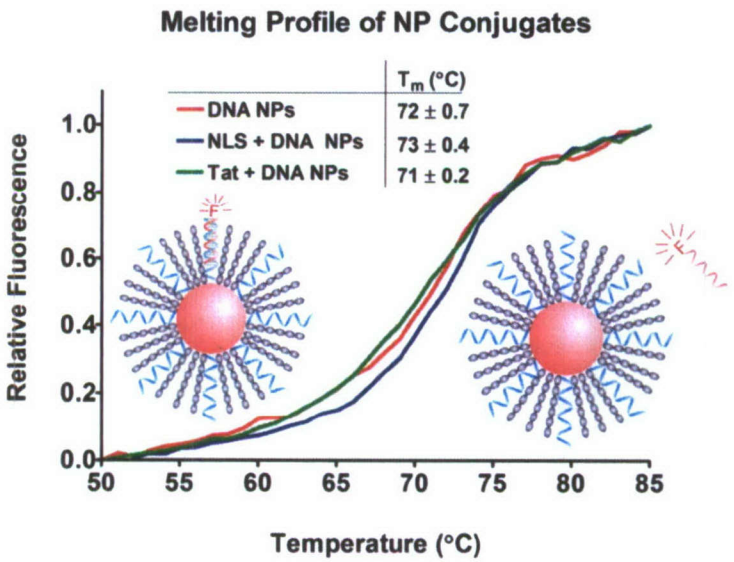

Figure 12. Melting profiles of nanoparticles co-loaded with peptide-DNA compared to nanoparticles loaded with DNA. The scheme represents fluorescein-labeled DNA melting off the complementary DNA bound to the gold nanoparticles co-loaded with peptide-DNA (**Blue** and **Green**). The DNA alone control contained the same DNA sequence with no peptides (**Red**).

In order to test the antisense efficacy of these nanoparticle conjugates, HeLa cells were treated with either different concentrations of nanoparticles functionalized with oligonucleotides and peptides or controls. After 48 hours, the cells were collected, counted and their protein content analyzed by Western blots. Nanoparticles functionalized with oligonucleotides reduced target protein expression by 53% after 48 hours, whereas nanoparticles containing both peptides and antisense oligonucleotides reduced target protein concentration by 75% and 78 % for the Tat and NLS peptides, respectively. For the control nanoparticles no appreciable decrease in target protein was observed (Figure 13). These data strongly indicate that the peptides on the nanoparticle surface are contributing to the increase in antisense efficacy of the gold nanoparticle system.

To conclude, these results demonstrated a significant advance in the use of nanoparticle-biomolecule conjugates for intracellular applications. It could be shown that (1) gold nanoparticles can be functionalized with two different biomolecules, (2) the density of each molecule can be easily controlled, and (3) both functionalities remain active *in vitro* and *in vivo*. This research will advance the use of gold nanoparticle conjugates in biological studies and will provide a platform for further improvements.

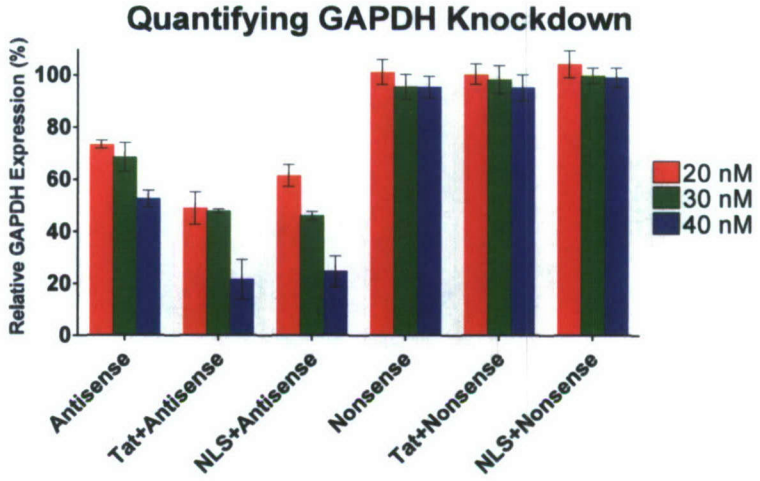

Figure 13. Relative decrease in GAPDH expression in HeLa cells 48 hours after addition of nanoparticles. Hela cells not treated with antisense nanoparticles served as a control. At 40nM concentration, nanoparticle conjugates functionalized with antisense oligonucleotide plus Tat or NLS peptides decreased GAPDH expression by 78 ± 13% and 75 ± 10%, respectively. For comparison antisense nanoparticles alone produced a 53±7% decrease.

PERSONNEL SUPPORTED

Postdocs:	**% of Salary Provided by Grant**
2005	
Nat Rosi	100%
2006	
Nat Rosi	50%
2007	
Jacob Ciszek	8%
Gengfeng Zheng	9%
Graduate Students:	
2005	
Emma Kate Payne	100%
2006	
Emma Kate Payne	92%
Xiaoyang Xu	8%
Fengwei Huo	8%
Andrew Senesi	8%
2007	
Xiaoyang Xu	90%
Fengwei Huo	45%
Andrew Senesi	42%

PUBLICATIONS

1. Rosi, N.; Thaxton, C.S.; Mirkin, C.A. "Control of Nanoparticle Assembly Using DNA-Modified Diatom Templates" Angew. Chem. Int. Ed. **2004**, *116*, 5616-5619.
2. Payne, E.K.; Rosi, N.L.; Xue, C.; Mirkin, C.A. "Sacrificial Bio-Templates for the Formation of Nanostructured Metallic Microshells" *Angew. Chem.* **2005**, *44*, 2-4.
3. Huo, F.; Lytton-Jean, A.K.R.; Mirkin, C.A. "Asymmetric Functionalization of Nanoparticles Based on Thermally Addressable DNA Interconnects," *Adv. Mater.*, **2006**, *18*, 2304-2306
4. Xu, X.-Y.; Rosi, N.L.; Wang, Y.; Huo, F.; Mirkin, C.A. "Asymmetric Functionalization of Gold Nanoparticles with Oligonucleotides," *J. Am. Chem. Soc.*, **2006**, *128*, 9286-9287.
5. Hurst, S.J.; Payne, E.K.; Qin, L.; Mirkin, C.A. "Multi-Component One-Dimensional Nannostructures," *Angew. Chem.*, **2006**, *46*, 2672-2692.

PRESENTATIONS AT MEETINGS, CONFERENCES, AND SEMINARS

1. AFOSR Biomimetic Program, San Diego CA; "Ultrasensitive and Selective Chip Based Detection of DNA" (2005).
2. Nanoscience Seminar Series, Duke University, Durham NC; "Massively Parallel Dip Pen Nanolithography", "Synthetic Supramolecular Allosteric Catalysts" (2005).
3. 228th ACS National Meeting, San Diego, CA; "Anisotropic Nanostructures: Synthesis, Assembly, and Function," "Biobarcode Assay: PCR-Like Sensitivity for Proteins, Nucleic Acids, and Small Molecules," "Nanoarrays for Probing Fundamental Issues in Nanoscience, Chemistry, and Biology," "Living Templates for the Assembly of Nanoparticle Building Blocks into Functional Architectures" (2005).
4. AACC Oak Ridge Conference, Baltimore, MD; "The Bio Barcode Assay: Towards PCR-Like Sensitivity for Proteins, Nucleic Acids, Small Molecules, and Metal Ions" (2005).
5. Princeton University, Princeton, NJ; "Encoded Nanostructures for use in Biodiagnostics"(2005).
6. BioMEMS Seminar, MIT, Boston, MA; "The Bio-Barcode Assay: PCR-like Sensitivity for Proteins, Nucleic Acids, and Small Molecules" (2005).
7. Gordon Research Conference: 3Chem of Supramolecules, Colby College, ME; "Supramolecular Allosteric Catalysts" (2005).
8. Gordon Research Conference: Bioorganic Conference, Andover, NH; "The Bio Barcode Assay: Towards PCR-like Sensitivity for Proteins" (2005).
9. BIO2005, Philadelphia, PA; "Big Academia, A Key to Small Science" (2005).
10. Gordon Research Conference: Organometallic, Newport RI; "Allosteric Catalysts Made Possible via the Weak-Link Approach to Supramolecular Coordination Chemistry" (2005).
11. UCLA ICCOS XVII Conference, Los Angeles, CA; "The Chemistry and Physical Properties of Self-Organized Nanomaterials" (2005).
12. 230th ACS National Meeting, Washington, DC; "Bio-Inspired Assembly of Mesoscopic Building Blocks into Functional Architectures," "New Frontiers in Ultrasensitive Analysis: Nanobiotech, Single Molecule Detection, and Single Cell Analysis," "Bio-Programmed Assembly of Nanostructured Materials into Functional Architectures," "Biological Nanoarrays" (2005).

13. AACI 2005 Annual Meeting, Washington, D.C.; "The Bio-Barcode Assay and Its Implications in Cancer Research" (2005).
14. Dupont Meeting, Wilmington, DE; "The Bio-Barcode Assay and Its Implications in Cancer Research" (2005).
15. LUX Executive Summit, Cambridge, MA; Panel Member "Nanotech Innovation Outlook: Leading Scientists Identify Game-Changing Technologies" (2005).
18. MIT Materials Seminar Series, Cambridge, MA; "Anisotropic Nanostructures: Synthesis Challenges, Assembly, and Biomedical Applications" (2005).
19. NanoCommerce/SEMI NanoForum, Chicago, IL; "A Vision for Nanoscience and Nanotechnology" (2005).
20. Centers of Cancer Nanotechnology Excellence Kickoff Meeting, Bethesda, MD; "Development of Barcode Assays for Detection of Ovarian Cancer" (2005).
21. MRS 2005 Fall Meeting, Boston, MA; "Anisotropic Nanostructures: Synthesis, Assembly, and Function" (2005).
22. Pacifichem 2005 Congress, Honolulu, HA; "The Biobarcode Assay", "The Unusual Properties of Nanoparticles", "On-Wire Lithography (OWL)" (2005).
23. 2005 AFOSR Biomimetic, Biomaterial and Biointerfacial Sciences Program Review, Duck Key, FL; "DURINT-01: Ultrasensitive and Selective Chip-Based Detection of DNA", "Diatomaceous, Fungal and Bacterial Building Blocks for Material Synthesis" (2006).
24. PittCon Conference, Orlando, FL; "Massively Parallel Dip-Pen Nanolithography", "Ultrasensitive and Multiplexed Protein Detection with Nanoparticle-based Bio-barcodes" (2006).
25. Burnham Institute Symposium, La Jolla, CA; "The Bio-Barcode Assay: Towards PCR-like Sensitivity for Proteins, Nucleic Acids, Small Molecules, and Metal Ions" (2006).
26. Center for Nanoscale Materials Users Meeting: Argonne National Laboratory, Chicago, IL; "Biomolecule Directed Assembly" (2006).
27. Burgenstock Conference, Burgenstock, Switzerland; "Nanostructures in Chemistry and Biodiagnostics" (2006).
28. ExxonMobil Longer Range Research Meeting on Nanotechnology, ExxonMobil Corp., Paulsboro, NJ; "The Bio-Barcode Assay: Towards PCR-like Sensitivity for Proteins, Nucleic Acids, Small Molecules, and Metal Ions" (2006).
29. Bionanotechnology for Medical Applications Meeting, Northwestern University, Chicago, IL; "The Bio-Barcode Assay: Towards PCR-like Sensitivity for Proteins, Nucleic Acids, Small Molecules, and Metal Ions" (2006).
30. Yale Chemical Biology Symposium, Yale University, New Haven, CT; "New Nanotechnological Tools for Studying Biological Systems at the Single Particle Level" (2006).
31. UCLA School of Medicine, Los Angeles, CA; "The Bio-Barcode Assay: Towards PCR-like Sensitivity for Proteins, Nucleic Acids, Small Molecules, and Metal Ions" (2006).
32. HSARPA Performers Conference, Monterey, CA; "Encoded Nanostructures for the Analysis of Bioterrorism Threats" (2006).
33. Gordon Research Conference: Nanostructure Fabrication, Tilton, NH; "Unconventional Nanofabrication Technologies" (2006).
34. AACC Annual Meeting, Chicago, IL; "Nanotechnological Tools That Will Impact Molecular Diagnostics" (2006).

35. BASF Meeting, Ludwigshafen, Germany; "Massively Parallel Dip-Pen Nanolithography" (2006).
36. ICN+T 2006: International Conference on Nanoscience and Technology, Basel, Switzerland; "Massively Parallel Dip-Pen Nanolithography" (2006).
37. GRC 2006 Bioelectrochemistry Conference, Aussois, France; "Bio Barcode Amplification PCR-like Sensitivity for Proteins" (2006).
38. TNT 2006 Conference, Grenoble, France; "Novel Approaches to Nanostructure Assembly and Nanofabrication" (2006).
39. MESA/Institute for Nanotechnology, University of Twente, Enschede, Netherlands; "Unconventional Approaches to Nanofabrication" (2006).
40. GRC 2006 Biointerface Science, Les Diablerets, Switzerland; "Bio-Barcode Assay" (2006)
41. Pauling Symposium, Western Washington University, Bellingham, WA, "The Evolution of Massively Parallel Dip-Pen" (2006).
42. DARPA, San Francisco, CA; "Tip-Based Nanofabrication for Defense Applications" (2006)
43. MRS Fall Meeting, Boston, MA; "Bionanoarrays Prepared by Massive Parallel Dip-Pen Nanolithography" (2006).
44. NSF/NIST/NIBIB Workshop, Enhancing Innovation and Competitiveness, Arlington, VA; "Nanotechnology, Academic Response" (2006).
45. Office of Naval Research (ONR), Materials for Forensic Sensing (MFS) Workshop, Arlington, VA; "The Multiplexed Bio-Barcode Assay" (2006).
46. 2007 AFOSR Biomimetic, Biomaterial and Biointerfacial Sciences Program Review, Hawk's Cay, FL; "Surface-Templated Bio-Inspired Synthesis and Fabrication of Functional Materials", "Ultra-sensitive and Selective Chip-Based Detection of DNA", "Diatomaceous, Fungal and Bacterial Building Blocks in Material Synthesis" (2007).
47. Gordon Research Conference, Chemical and Biological Terrorism Defense, Ventura, CA; "Nanotechnology" (2007).
48. Nanyang Technological University, Singapore; "The Evolution of Massively Parallel Dip-Pen Nanolithography" (2007).
49. Pittcon Symposium, Chicago, IL; "Anisotropic Nanostructures: Synthesis, Assembly and Function", "Gold Nanoparticle Delivery Agents", Controlling Plasmons with On-Wire Lithography" (2007).
50. Murray Lecture, Department of Chemistry, University of Missouri, St. Louis, MO; "Nanoparticles for Diagnostics and Therapeutics" (2007).
51. Donaldson Lecture, University of Minnesota, Minneapolis-St.Paul, MN; "Massively Parallel Dip-Pen Nanolithography Towards Combinatorial Nanotechnology," and "The Antisense Nanoparticle" (2007).
52. Arthur M. Sackler Colloquia, National Academy of Sciences, Washington, DC; "Nanotechnological Approaches to Amplification in Chemical and Biological Systems." (2007)
53. Kavli Nanoscience Colloquia Series, California Institute of Technology, Pasadena, CA; "The Antisense Nanoparticle", "Commercializing Advances in Nanotechnology: Challenges and Opportunities" (2007).

54. NanoMaterials for Defense Applications Symposium: Accelerating the Transition, San Diego, CA: "Nanostructure Self-Assembly and Nanoparticles for Gene Regulation" (2007).
55. Colloquium, University of Cincinnati, Department of Chemistry, Cincinnati, OH; "Nanochemistry Driving Nanotechnology: From High Resolution Lithographic Methods to Powerful New Biodiagnostic Tools" (2007).
56. The Young(-ish) Giants of Chemistry, A Symposium to Celebrate Fraser Stoddart's 65th Birthday Edinburgh, Scotland; "The Antisense Nanoparticle" (2007).
57. Keynote Lecture, MIT-Harvard University CCNE Retreat, Massachusetts General Hospital, Center for Molecular Imaging Research, Charlestown, MA (2007).
58. Japan-US Joint Symposium on Chemistry Coordination Space, Northwestern University, Evanston, IL; "Allosteric Supramolecular Systems" (2007).
59. Gordon Research Conference: Nucleosides, Nucleotides, and Oligonulceotides, Salve Regina University, Newport, RI; "Non-enzymatic Approaches to Amplification in Biological Detection Systems" (2007).
60. 20th International Vacuum Nanoelectronics Conference, Chicago, IL; "Massively Parallel Dip-Pen Nanolithography: Towards a Desktop Fab" (2007).
61. Gordon Research Conference: Chemical Sensors & Interfacial Design, Salve Regina University, Newport, RI; "The Oligonucleotide Nanoparticle Conjugate" and "The Antisense Particle" (2007).
62. 234th ACS National Meeting, Boston, MA; "Nanotechnology: New Chemistry, New Materials, New Properties, New Technological Capabilities", "The Oligonucleotide Nanoparticle Conjugate: A Versatile Probe in Biodetection", and "Nanoparticle Antisense and siRNA Delivery Agents" (2007).
63. MoleApps PI review meeting, Arlington, VA; "Nanotechnology Support Tools for MoleApps: Sensing/Enabling" (2007).
64. Colloquium, University of Virginia, Charlottesville, VA; "The Oligonucleotide Nanoparticle Conjugate," and the "Antisense Nanoparticle" (2007).
65. MicroTAS, 11th International Conference on Miniaturized Systems for Chemistry and Life Sciences, Plenary Lecture, Paris, France; "Nanotechnological Approaches to Amplification in Biological and Chemical Detection Systems" (2007).
66. Phillips Lectures, University of Pittsburgh, Pittsburgh, PA; "Unconventional Ways of Lithographically Generating and Studying Nanostructures," and "The Oligonucleotide Gold Nanoparticle Conjugate and the Antisense Nanoparticle" (2007).
67. The President's Research Seminar, Memorial Sloan Kettering Cancer Center, New York, NY; "Nanostructures in Medicine" (2007).
68. Yale University, Department of Chemistry, New Haven, CT; "Approaches to Amplification in Chemical and Biological Detection Systems" (2007).
69. MRS Fall Meeting, Boston, MA; "Nanodisk Codes" (2007).
70. NSF Nanoscale Science and Engineering Grantees Conference, Arlington, VA; "The Future and Legacy of the NSEC Program" (2007).

CONSULTATIVE/ADVISORY FUNCTIONS

Mirkin consults for Nanosphere, Inc. and NanoInk, Inc, Kirkland & Ellis LLP, NextGen Aeronautics, and Fuji Film.

INVENTIONS AND PATENT DISCLOSURES

1. Chad A. Mirkin, Fengwei Huo, Abigail Lytton-Jean, "Asymmetric Functionalization of Nanoparticles Based on Thermally Addressable DNA Interconnects," NU 26089.
2. Chad A. Mirkin, Xiaoyang Xu, Nathaniel Rosi, "Asymmetric Functionalization of Nanoparticles with Oligonucleotides," NU 26090.
3. Chad A. Mirkin, Jae-Wong Jang, Daniel Maspoch, "A Molecular Eraser for Dip-Pen Nanolithography," US Prov. Patent Application # 60/880,795.
4. Chad A. Mirkin, Rafael A. Vega, Steven Lenhert, Ling Huang, Dorota Rozkiewicz, "The Use of Phospholipids as a Universal Ink Carrier in Dip-Pen Nanolithography for Patterning Unmodified Biomolecules," US Prov. Patent Application # 60/945,164.
5. Chad A. Mirkin, Rafael A. Vega, Clifton K.-F. Shen, Daniel Maspoch, Jessica Robach, Robert Lamb, "Monitoring Single Cell Infectivity from Virus Particle Nanoarrays Fabricated by Parallel Dip-Pen Nanolithography," US Prov. Patent Application # 60/952,753.
6. Chad A. Mirkin, Andrew Senesi, "The Use of Chemical Additives to Regulate the Difusión Rate for Dip-Pen Nanolithography of Biomolecules Using Agarose as a Carrier Matrix," NU 28024.

HONORS/AWARDS

2007 iCON Innovator of the Year Award
2007 Elected Alumni Fellow, Pennsylvania State University
2007 In Cites Top 10 Most Cited Chemists in the World (#5)
2006 Elected into Phi Beta Kappa, Dickinson College
2006 In Cites Top 10 Most Cited Chemists in the World (#10)
2005 In Cites Top 100 Most Cited Chemists in the World (#19)
2005 Elected to the Board of Trustees, Dickinson College